

# Inhibitory Effect of *Lygodium* Root on the Cytochrome P450 3A Enzyme in vitro and in vivo

This article was published in the following Dove Press journal:  
*Drug Design, Development and Therapy*

Yunfang Zhou<sup>1,\*</sup>

Ailian Hua<sup>2,\*</sup>

Quan Zhou<sup>1</sup>

Peiwu Geng<sup>1</sup>

Feifei Chen<sup>1</sup>

Lianhe Yan<sup>1</sup>

Shuanghu Wang<sup>1</sup>

Congcong Wen<sup>3</sup>

<sup>1</sup>The Laboratory of Clinical Pharmacy, The Sixth Affiliated Hospital of Wenzhou Medical University, The People's Hospital of Lishui, Lishui, Zhejiang 323000, People's Republic of China; <sup>2</sup>Department of Pharmacy, The First People's Hospital of Yuhang District, Hangzhou, Zhejiang 311100, People's Republic of China; <sup>3</sup>Laboratory Animal Centre, Wenzhou Medical University, Wenzhou, Zhejiang 325027, People's Republic of China

\*These authors contributed equally to this work

**Purpose:** The aim of the present study was to investigate the interactions of the main components of *Lygodium* root (ie, p-coumaric acid, acacetin, apigenin, buddleoside and Diosmetin-7-O-β-D-glucopyranoside) with cytochrome P450 3A enzyme activity both in vitro and in vivo.

**Methods:** In vitro inhibition of drugs was assessed by incubating rat liver microsomes (RLMs) with a typical P450 3A enzyme substrate, midazolam, to determine their 50% inhibitory concentration (IC<sub>50</sub>) values. For the in vivo study, healthy male Sprague Dawley rats were consecutively administered acacetin or apigenin for 7 days at the dosage of 5 mg/kg after being randomly divided into 3 groups: Group A (control group), Group B (acacetin group) and Group C (apigenin group).

**Results:** Among the five main components of *Lygodium* root, only acacetin and apigenin showed inhibitory effects on the cytochrome P450 3A enzyme in vitro. The IC<sub>50</sub> values of acacetin and apigenin were 58.46 μM and 8.20 μM, respectively. Additionally, the in vivo analysis results revealed that acacetin and apigenin could systemically inhibit midazolam metabolism in rats. The T<sub>max</sub>, AUC<sub>(0-t)</sub> and C<sub>max</sub> of midazolam in group B and group C were significantly increased (*P*<0.05), accompanied by a significant decrease in V<sub>Z/F</sub> and CL<sub>Z/F</sub> (*P*<0.05).

**Conclusion:** Acacetin and apigenin could inhibit the activity of the cytochrome P450 3A enzyme in vitro and in vivo, indicating that herbal drug interactions might occur when taking *Lygodium* root and midazolam synchronously.

**Keywords:** *Lygodium* root, drug–drug interactions, rat liver microsomes, midazolam, metabolism

## Introduction

*Lygodiumjaponicum* (Thunb.) Sw., also named Hai Jia Sha, belongs to the Lygodiaceae family 1, which is endemic to southern and southwestern China. This species is a perennial plant, and roots of several species of this genus are commonly used in traditional Chinese medicine to treat hepatitis and dysentery.<sup>1</sup> According to the medication habits of SHE nationality, *Lygodium* root has the functions of heat-clearing, detoxifying, dispersing swelling and detumescence. To date, a number of monomers have been extracted from *Lygodium*, including flavonoids, triterpenes, unsaturated hydrocarbons, organic acids, ketones, and non-terpene alcohols. Apigenin, found in many plants, is a natural product belonging to the flavone class and is the aglycone of several naturally occurring glycosides.<sup>2,3</sup> Apart from its traditional anti-inflammatory effect, acacetin has a variety of biological activities, such as antioxidant and anti-tumor activities.<sup>4-6</sup> The main active

Correspondence: Shuanghu Wang  
The Laboratory of Clinical Pharmacy, The Sixth Affiliated Hospital of Wenzhou Medical University, The People's Hospital of Lishui, Lishui 323000, Zhejiang, People's Republic of China  
Email wangshuanghu@lsu.edu.cn

Congcong Wen  
Laboratory Animal Centre, Wenzhou Medical University, Wenzhou, Zhejiang 325027, People's Republic of China Tel/ Fax +865782780081  
Email bluce494949@163.com

component of *Lygodium* root is p-coumaric acid, which exhibits multiple antioxidant activities by regulating the expression of cardioprotective antioxidant enzymes, such as superoxide dismutase (SOD), glutathione (GSH), and catalase (CAT).<sup>7</sup> In addition, it also possesses anti-inflammatory,<sup>8,9</sup> antineoplastic,<sup>10</sup> antimicrobial<sup>11</sup> and neuroprotective properties.<sup>12</sup>

Cytochrome P450 is the most important drug-metabolizing enzyme in the human body, and it can metabolize more than 70% of drugs commonly used in clinic.<sup>13–15</sup> The human CYP enzyme includes 18 families and 44 subfamily members, of which CYP3A4 is the most abundantly expressed drug metabolism enzyme in the human liver, comprising, on average, approximately 30% of the microsomal P450 pool. CYP3A4 is also the most important drug-metabolizing enzyme in adult humans owing to its extraordinarily broad substrate spectrum. The CYP3A4 enzyme plays a major role in the oxidative metabolism of approximately 30–40% of clinically used drugs.<sup>16</sup> The enzyme activity of CYP3A4 shows wide inter-individual variability, up to 60-fold,<sup>17</sup> and this enormous variation in drug metabolism is mainly due to a combination of several factors, such as genetic polymorphisms, regulation of gene expression and interactions with drugs or environmental chemicals.<sup>18</sup>

The incidence of drug–drug interactions (DDIs) and herb–drug interactions (HDIs) can lead to beneficial or severe and sometimes lethal clinical outcomes.<sup>19,20</sup> In contrast to DDIs, the study of HDIs remains challenging due to the inherent physicochemical complexity of herbs and their multi-target modulatory potential.<sup>21</sup> Moreover, patients with chronic diseases are likely to be treated with multiple drugs, including herbal medicines, thereby increasing the risk of drug–drug interactions.<sup>22</sup> For example, *Lygodium* root was widely used to treat hepatitis in some ethnic minorities in China. Midazolam was a medication used for anesthesia, procedural sedation,<sup>23,24</sup> insomnia, and severe agitation,<sup>25</sup> which could induce drowsiness, decrease anxiety, and cause a loss of ability to create new memories.<sup>26</sup> Therefore, when *Lygodium* root and midazolam are taken together, clinical herb–drug interactions may appear.

In this paper, a sensitive and reliable method with ultra-high-performance liquid chromatography coupled with triple-quadrupole electrospray tandem mass spectrometry (UPLC-MS/MS) was developed to simultaneously quantify five bio-active components (ie, p-coumaric acid, acacetin, apigenin, buddleoside, and Diosmetin-7-O- $\beta$ -

D-glucopyranoside) in one analysis. A DDI study of midazolam with acacetin or apigenin in vitro and in vivo was successfully described in this paper. Our data indicated that two main components of *Lygodium* root, AC and AP, had a strong influence on midazolam metabolism. Therefore, more attentions might be paid when taking *Lygodium* root and midazolam synchronously in clinic and our developed methods could be applied for the safety and toxicity evaluation of *Lygodium* root in clinic.

## Materials and Methods

### Chemicals and Reagents

*Lygodium* (*L. microstachyum* Desv. species) root was provided by SHE Nationality Medical Research Institute of The People's Hospital of Lishui. P-coumaric acid (PCA), acacetin (AC), apigenin (AP), buddleoside (BU) and Diosmetin-7-O- $\beta$ -D-glucopyranoside (DDG) (Figure 1) were purchased from MUST Biotech (Chengdu, China). Midazolam (MDZ) and hydroxy-midazolam (OHMDZ) were purchased from Toronto Research Chemicals (Toronto, Canada). HPLC grade methanol and acetonitrile were purchased from Fisher Scientific Co. (Fair Lawn, New Jersey, USA). Deionized water was produced by the Milli-Q system (Millipore, Bedford, MA, USA). The remaining conventional chemical reagents were all purchased from Beijing Chemical Reagents Company (Beijing, China). BCA Protein Assay Kit was supplied by Pierce (Thermo Scientific, USA). Coenzymes NADPH was purchased from Roche Diagnostics GmbH (Mannheim, Germany).

### Animals

Male Sprague Dawley rats (200–250 g) were supplied by the Experimental Animal Center of Wenzhou Medical University. They were placed in rooms with lights in the 12–12 day and night cycle. All rats were fed a standard rodent diet and consumed tap water ad libitum, except during the 12-hrs fasting period prior to the pharmacokinetic study. All experimental procedures and protocols were reviewed and approved by the Animal Care and Use Committee of Wenzhou Medical University (NO. wyd2017-0010) and were in accordance with the Guide for the Care and Use of Laboratory Animals.

### Preparation and Fermentation of *Lygodium* Root

*Lygodium* root was provided by the SHE Nationality Medical Research Institute of The People's Hospital of Lishui. A quantity of 50 g dried *Lygodium* root powder

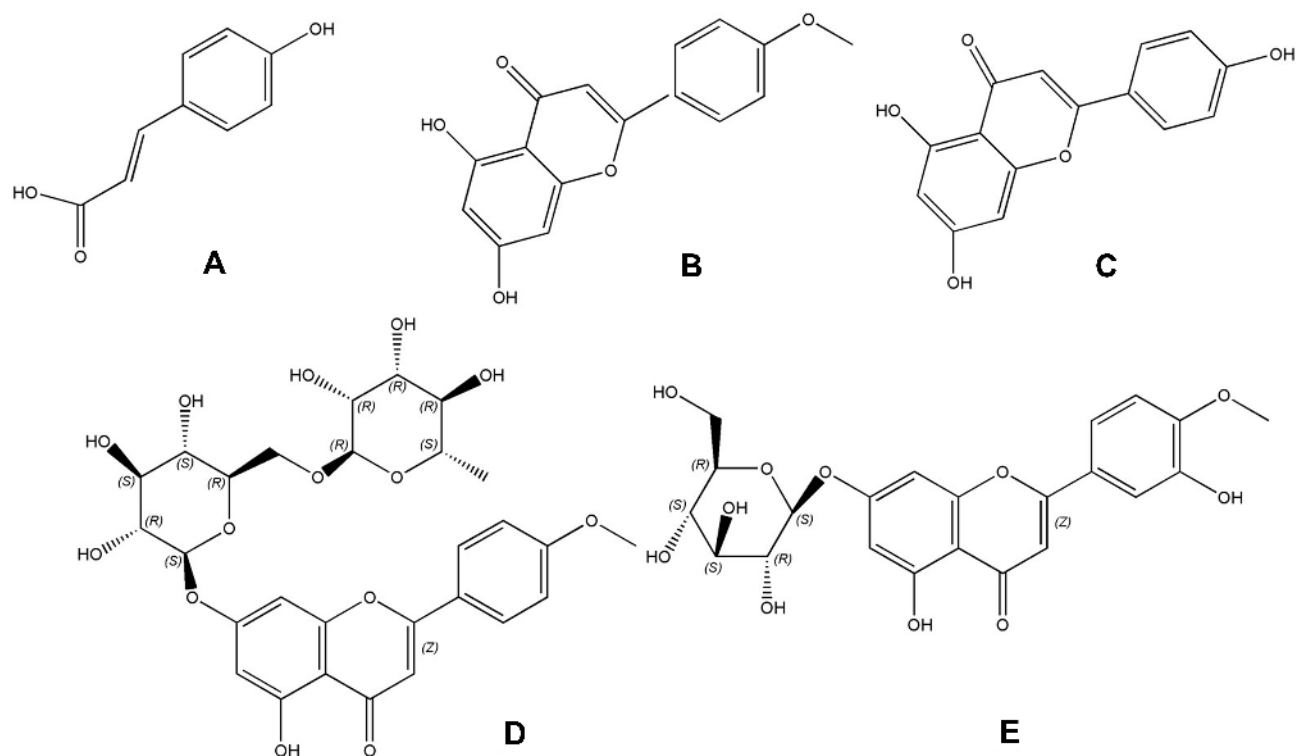


**Figure 1** Structures of five typical compounds: PCA (A), AC (B), AP (C), BU (D) and DDG (E).

was first soaked in a twice volume of water for 1 hr and then heated to decoct for 1 hr, followed by filtering with filter paper. A second decocting was performed for one additional hour by adding a volume of water twofold larger than the filter residue. Finally, two decocted filtrates were combined to obtain the final crude drug solution with a concentration of 2 g/mL. A volume of 1 mL decoction and 50 mL methanol-water mixed solution (1:1) was mixed together in a triangular flask and treated with ultrasound (200 W, 40 kHz) for 30 mins. Then, the methanol-water mixed solution (1:1) was filled up to a specific volume, followed by filtration with a 0.22  $\mu\text{m}$  membrane (Millipore, Bedford, MA, USA).

### Simultaneous Quantification of the Main Compounds in *Lygodium* Root

Five quantifications of the main compounds, PCA, AC, AP, BU and DDG, were dissolved in the methanol-water mixed solution (1:1). A UPLC-MS/MS method for the simultaneous determination of PCA, AC, AP, BU and DDG in *Lygodium* root was successfully developed. An ACQUITY UPLC BEH C18 (50 mm  $\times$  2.1 mm, 1.7  $\mu\text{m}$ ) column was used for the separation of the five compounds

with a gradient elution system consisting of acetonitrile and water with 0.1% formic acid.

The triple-quadrupole mass spectrometer was operated in the positive electrospray ionization mode with an ESI interface. Capillary voltage was set at 1 kV, and cone voltages were 25, 55, 60, 40 and 35 V for PCA, AC, AP, BU and DDG, respectively. Collision energy was set at 11, 35, 30, 31 and 20 V for PCA, AC, AP, BU and DDG, respectively. Source and desolvation temperatures were both 150°C. The desolvation gas flow was 1000 L/h, and the cone gas (nitrogen) flow was 50 L/h. The multiple reaction monitoring modes of 164.96–146.99 m/z for PCA, 285.09–242.06 m/z for AC, 271.09–153.01 m/z for AP, 593.23–285.09 m/z for BU and 463.12–301.02 m/z for DDG were used for quantitative analysis, with a scan time of 0.063 s per transition. Masslynx 4.1 software (Waters Corp, Milford, MA, USA) was used for data processing.

### Standard Sample Preparation

A quantity of 10 mg of the standard midazolam and hydroxy-midazolam was accurately weighed and dissolved in methanol in a 10 mL volumetric flask at a concentration of 1 mg/mL. The midazolam and hydroxy-midazolam stock solutions were stored at 4°C until use. A quantity

of 5 mg diazepam (as the internal standard, IS) was accurately weighed in a 10 mL volumetric flask and prepared with a methanol-water solution at a concentration of 500  $\mu\text{g}\cdot\text{mL}^{-1}$  as a stock solution. The working solution (500  $\text{ng}\cdot\text{mL}^{-1}$ ) was diluted with methanol.

Separate 5 mg quantities of PCA, AC, AP, BU and DDG were accurately weighed. Those samples were set in a 10 mL volumetric flask and were dissolved in a methanol-water solution. The stock solutions of PCA, AC, AP, BU and DDG were 500  $\mu\text{g}\cdot\text{mL}^{-1}$ .

## Plasma Sample Preparation

Plasma samples were treated with precipitation. After thawing, 20  $\mu\text{L}$  diazepam was added to 100  $\mu\text{L}$  samples and vortex-mixed for 10 s. Afterward, 100  $\mu\text{L}$  acetonitrile was added and was vortex-mixed for 30 s. Samples were centrifuged at 13,000 r/min for 1 min. The supernatant was then injected into a vial.

## Preparation and Protein Concentration Determination of RLMs

The RLMs were prepared in our laboratory according to a standing protocol. Rat livers were removed after perfusion with normal saline (0.9%) after the rats were anesthetized with 0.6% Amytal sodium (0.65 mL/100 g). A quantity of 3 g liver was accurately weighed and homogenized in an ice bath. The liver homogenate was prepared and centrifuged in 9000 g for 30 mins at 4°C. The supernatant was removed and centrifuged again at 4°C and 105,000 g for 60 mins. After centrifugation, the supernatant was discarded to obtain a pink precipitate, which was resuspended in 0.15 mol KCl-PBS solution (containing 0.25  $\text{mol}\cdot\text{L}^{-1}$  sucrose). Protein concentrations were determined by the Micro BCA Protein Assay Kit.

## Optimization of the Incubation Conditions and Sample Preparation

To simplify the process of incubation optimization, the concentrations of RLMs and midazolam were fixed. The reaction was terminated with different buffer solutions, different volumes of microsomes and different time points to determine the amount of metabolites and to guarantee the linear formation of midazolam metabolites. The optimized incubation conditions (ie, buffer, microsome volume and time) were chosen for the subsequent enzyme kinetic assay and inhibition study. First, 100 mM PBS (pH=7.4) and 100 mM Tris-HCl buffer (pH=7.4) was selected in the parallel

incubation system with comparable amounts of hydroxymidazolam. Second, incubation time points of 5, 10, 20, 30, 40, 50 and 60 mins were selected in the parallel incubation system. The number of microsomes should have a linear relationship with the amount of metabolite that reacted, and the appropriate line segment should be chosen to select the number of microsomes. Finally, 1, 2, 3, 4 and 5  $\mu\text{L}$  of RLMs were used in the parallel incubation system. Incubations were initiated following a 5-mins pre-incubation in a shaking water bath at 37°C. Then, NADPH was added to start the reaction. The reaction was terminated by cooling to -80°C immediately after 20 min of incubation. Then, 400  $\mu\text{L}$  acetonitrile and 20  $\mu\text{L}$  diazepam (the IS, 50  $\text{ng}/\text{mL}$ ) were added. After vortex mixing for 30 s, the tubes were centrifuged at 13,000 r/min for 5 mins, and the supernatant was collected. Each incubation sample study was performed in separate EP tubes, performed in triplicate and analyzed by UPLC-MS/MS. All the experimental data were expressed in mean  $\pm$  SD.

## In vitro CYP3A1 Inhibitor Screening and Inhibition Parameters

CYP3A1 inhibitor screening experiments were carried out in a 200  $\mu\text{L}$  incubation system containing midazolam solution with a final concentration of 10  $\mu\text{M}$  RLMs, 100  $\mu\text{M}$  PCA, AP, BU, and DDG or 35.2  $\mu\text{M}$  AC solution separately (ie, 3 tubes in parallel for each drug solution). Data were processed by using GraphPad Prism 5.0 software, and the percentage of remaining activity was plotted. The average residual activity of PCA, AP, BU, DDG, and AC was determined.

The inhibition assay was carried out with a 200  $\mu\text{L}$  incubation system containing 4  $\mu\text{L}$  of rat microsomes, 100 mM PBS (pH=7.4), 10  $\mu\text{M}$  midazolam (approximately the  $K_m$  of RLMs), AC or AP (0, 0.1, 0.5, 1, 2.5, 5, 10, 25, 50, or 100  $\mu\text{M}$ ) and 1 mM NADPH. All the experiments were carried out according to the sample preparation (ie, each drug concentration in parallel with three tubes). Data were processed using GraphPad Prism 5.0 software, and an IC<sub>50</sub> plot was drawn.

## In vivo Pharmacokinetic Studies

Eighteen Sprague Dawley rats, weighing 250  $\pm$  20 g, were divided into three groups with six mice in each group. Group A, as the control group, was given midazolam alone; group B (AC group) and group C (AP group) rats were consecutively administered AC or AP for 7 days at the dosage of 5 mg/kg. Midazolam was administered at a dose of 10 mg/kg. Blood samples were collected via tail vein into a 1.5 mL centrifuge

tube at 0.083, 0.25, 0.5, 1, 2, 3, 4, and 6 h. After centrifugation at 3000 rpm for 10 min, plasma samples were immediately separated from whole blood and frozen at  $-80^{\circ}\text{C}$  until analysis. Rats were allowed to drink water at 2 h after administration to ensure adequate blood volume. The pharmacokinetic parameters of the study were as follows: maximum plasma concentration ( $C_{\text{max}}$ ), maximum plasma time ( $T_{\text{max}}$ ), area under the plasma concentration–time curve (AUC), plasma clearance (CL), and half-life ( $t_{1/2}$ ). These parameters were processed by DAS software (Version 3.2.8, The People's Hospital of Lishui, China).

## Analytical Method

An ACQUITY UPLC BEH C18 (50 mm  $\times$  2.1 mm, 1.7  $\mu\text{m}$ ) column was used for the separation of midazolam and its metabolite. The mobile phase pumped with a gradient elution program consisting of (A) acetonitrile and (B) 0.1% formic acid was delivered at a flow rate of 0.4  $\text{mL}\cdot\text{min}^{-1}$ . The column heater was adjusted to  $40^{\circ}\text{C}$ . The internal standard was diazepam. Elution had a linear gradient, with the acetonitrile content changing from 20% to 40% between 0 and 2.8 min and increasing to 95% over 0.2 min. The acetonitrile content was maintained at 95% for 0.5 min and then decreased to 20% within 0.1 min and maintained at 30% for 0.4 min.

The electrospray ionization (ESI) was operated in a positive ion detection mode. The capillary voltage was 2.0 kV; ion source temperature,  $150^{\circ}\text{C}$ ; desolvation gas temperature,  $500^{\circ}\text{C}$ ; cone gas flow, 50 L/h; desolvation gas flow, 1000 L/h; argon flow, 0.15  $\text{mL}\cdot\text{min}^{-1}$ . The ionic reactions used for quantitative analysis were 326.02–290.99  $m/z$  for midazolam; 342.03–324.02  $m/z$  for hydroxy-midazolam; and 285.1–193.1  $m/z$  for the internal standard, diazepam. MassLynx (Version 4.1) software was used for data calculation and processing for the UPLC-MS/MS system.

Rigorous tests for selectivity, linearity, accuracy, precision, recovery, and stability were conducted according to the guidelines set by the United States Food and Drug Administration (FDA) and European Medicines Agency (EMA) to thoroughly validate the proposed bioanalytical method.<sup>27–33</sup> All the QC plasma samples were prepared on three consecutive days with six replicates.

## Data Analysis

This experiment used GraphPad Prism 5.0 software (GraphPad Software Inc., San Diego, CA) to calculate the enzyme kinetic parameters of midazolam, including the  $K_m$  value, the maximum reaction rate ( $V_{\text{max}}$ ), and the intrinsic clearance (IC50). A one-way analysis of variance was used

for comparisons between groups. The main pharmacokinetic parameters, such as  $t_{1/2}$ ,  $C_{\text{max}}$ , AUC, and  $C_{\text{L/F}}$  were statistically analyzed by using SPSS 17.0 software.  $P$ -values  $<0.05$  were considered to be statistically significant.

## Results

### Quantification of the Main Compounds in *Lygodium* Root

Representative MRM chromatogram of five compounds in *Lygodium* root decoction: BU, DDG, AC, AP and PCA is shown in Figure 2A. Calibration curves of standard components showed a strong linear relationship ( $R^2>0.9964$ ). The limit of quantification (LOQ) ranged from 0.1 to 0.2  $\text{ng/mL}$  (Table 1). The relative standard deviation (RSD) of the intraday and inter-day experiments ranged from 4.1% to 9.2% and 5.8% to 9.5%, respectively. The measured results of the recovery test varied from 96.19% to 101.99% with RSD values  $<9.21\%$ . A comparison of the amounts of the five compounds is listed in Table 2.

### Optimization of the Detection Method for Hydroxy-Midazolam and Midazolam by UPLC-MS/MS

A UPLC-MS/MS method for the quantification of midazolam, which is one of the typical probe drugs for CYP3A enzymes was developed in this study. As shown in Figure 2B, the retention times of hydroxy-midazolam, midazolam and the internal standard were 2.07 mins, 2.17 mins and 3.61 mins, respectively, with no detectable interference component in blank plasma.

Standard samples with serial concentrations of 0.5, 1, 2.5, 5, 10, 25, 50, and 100  $\text{ng}\cdot\text{mL}^{-1}$  hydroxy-midazolam and serial concentrations of 2.5, 5, 10, 25, 50, 100, 250 and 500  $\text{ng}\cdot\text{mL}^{-1}$  midazolam were prepared as the calibration curve. Results showed that the regression equation of hydroxy-midazolam was  $Y=0.00166842\cdot X+0.00850074$ , with  $r=0.9991$ , and its lowest limit of quantification was 0.1  $\text{ng}\cdot\text{mL}^{-1}$ . For midazolam, the regression equation was  $Y=0.00438818\cdot X+0.0193277$ , with  $r=0.9995$  and with a lower limit of quantitation of 0.5  $\text{ng}\cdot\text{mL}^{-1}$ .

Plasma concentrations of 0.5, 8, and 80  $\text{ng}\cdot\text{mL}^{-1}$  of hydroxy-midazolam and 4, 45, and 400  $\text{ng}\cdot\text{mL}^{-1}$  of midazolam were set as low, medium, and high-quality control points, respectively, in accuracy, precision, and recovery method validation. As shown in Table 3, the intraday and inter-day precision RSDs of hydroxy-midazolam and midazolam were both  $<11.8\%$ , and the matrix effect of the internal standard,

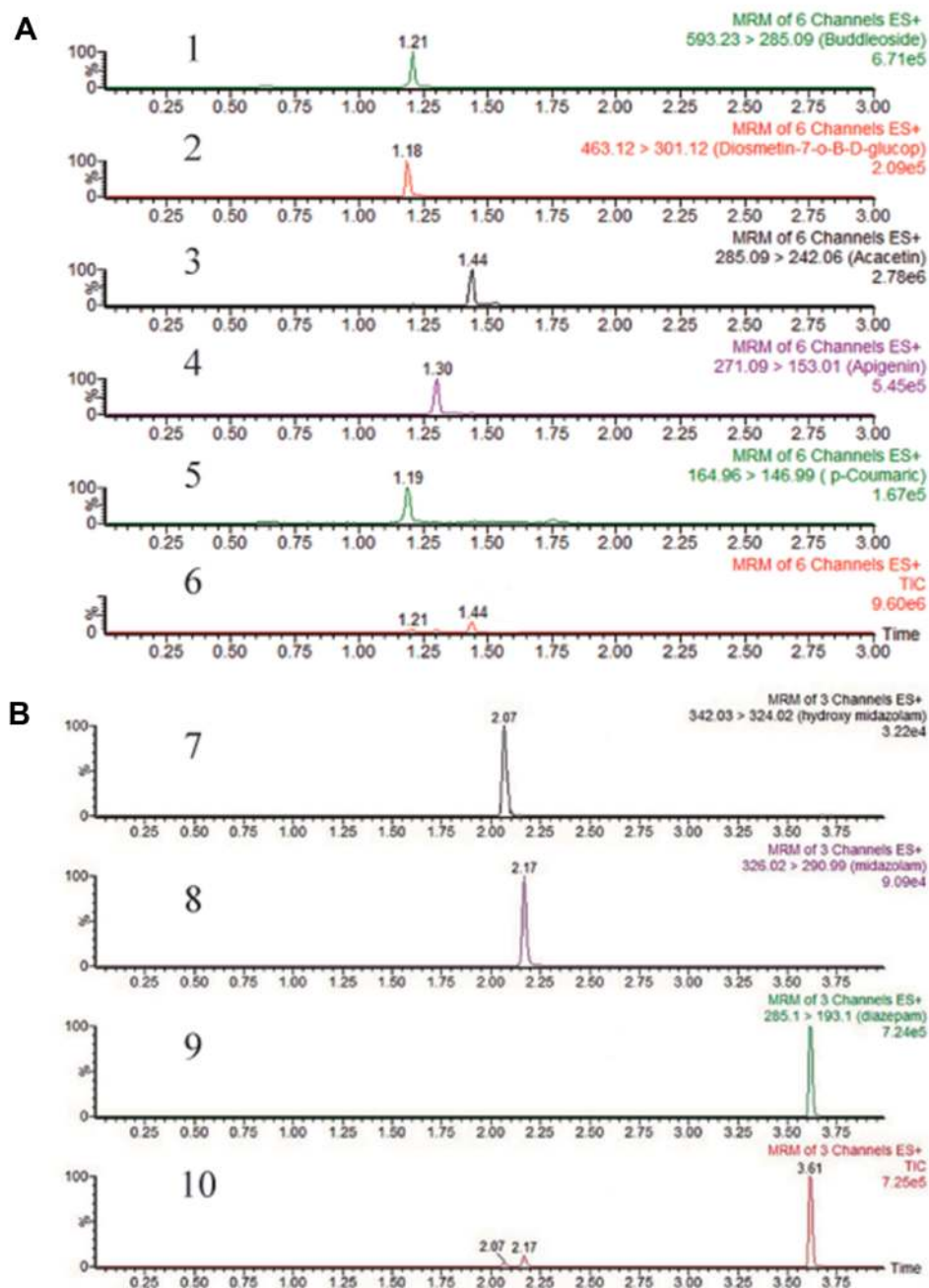


**Figure 2 (A)** Representative MRM chromatograms of five compounds in *Lygodium* root decoction: BU (1), DDG (2), AC (3), AP (4), PCA (5) and total ion chromatogram (6). **(B)** Representative MRM chromatograms of midazolam and hydroxyl-midazolam in rat plasma: hydroxyl-midazolam (7), midazolam (8), diazepam (9) and total ion chromatogram (10).

diazepam, was  $95.37 \pm 6.84\%$ , which indicated that the matrix does not substantially interfere with the detection.

Stability analysis revealed that no significant loss of hydroxy-midazolam or midazolam in rat plasma was observed at either low, medium or high concentrations (ie, 0.5, 8, 80  $\text{ng}\cdot\text{mL}^{-1}$  for hydroxy-midazolam and 4, 45, 400  $\text{ng}\cdot\text{mL}^{-1}$  for midazolam). Long-term, benchtop, room temperature storage, and freeze-thaw cycle

conditions were also evaluated. All stability tests of hydroxy-midazolam and midazolam in rat plasma indicated that the RSDs of the responses were less than 15%.

## Optimization of Incubation Conditions

The optimization of incubation conditions was carried out for three main aspects: reaction buffer, incubation time and microsome volume. The results revealed that the amount

**Table 1** Five Compounds Linear Regression Equation and Lower Limit of Quantification

Compounds	Regression Equation	Correlation Coefficient	LLOQ
PCA	67.0103*X+735.9	0.9964	0.1
AC	473.309*X +5888.32	0.9967	0.2
AP	124.686*X +1353.01	0.5595	0.1
BU	221.201*X +1098.37	0.9972	0.2
DDG	65.429*X+378.25	0.9965	0.1

**Abbreviations:** PCA, P-coumaric acid; AC, acacetin; AP, apigenin; BU, buddleioside; DDG, Diosmetin-7-O- $\beta$ -D-glucopyranoside.

**Table 2** Comparison of the Relative Amounts of Five Typical Compounds in *Lygodium* Root

Compounds	Concentration (ng/mL)	Amount (mg/g)	RSD (%)
PCA	94.527 $\pm$ 0.708	4.726 $\pm$ 0.036	0.749
AC	2.793 $\pm$ 0.162	0.140 $\pm$ 0.008	5.846
AP	16.743 $\pm$ 0.958	0.837 $\pm$ 0.048	5.72
BU	6.817 $\pm$ 0.09	0.341 $\pm$ 0.005	1.321
DDG	40.83 $\pm$ 0.566	2.042 $\pm$ 0.028	1.388

**Abbreviations:** PCA, P-coumaric acid; AC, acacetin; AP, apigenin; BU, buddleioside; DDG, Diosmetin-7-O- $\beta$ -D-glucopyranoside; RSD, relative standard deviations.

of hydroxy-midazolam in PBS was significantly higher than that in the Tris-HCl buffer. Within 5 to 30 min, the incubation time had a strong correlation ( $R^2 = 0.9941$ ) with the production rate of hydroxy-midazolam. The RLMs were well correlated with the production rate of midazolam ( $R^2 = 0.9976$ ) between 1 and 5  $\mu$ L. Based on these data, we selected 2  $\mu$ L of RLMs with a concentration of 0.665 mg/mL in PBS for 20 mins as the best condition for CYP3A enzyme kinetic studies. With this condition, we determined the kinetic parameters of midazolam for RLMs by adding 1, 2, 5, 10, 25, 50, and 100  $\mu$ mol of

midazolam to the 200  $\mu$ L incubation system. The  $V_{max}$  and  $K_m$  values for the rat liver microsomes were 83.24 ng  $(\text{min}\cdot\text{mg})^{-1}$  and 10.11  $\mu$ M, respectively.

### In vitro CYP3A1 Inhibitor Screening

When a *Lygodium* root extract solution was added to the optimized reaction system, the average residual activity of PCA, AC, AP, BU, and DDG were 101.86%, 39.27%, 29.64%, 90.01% and 99.89%, respectively (Figure 3A). These data indicated that only AP and AC had inhibitory effects on the CYP3A1 probe midazolam. As shown in Figure 3B and C, the  $IC_{50}$  values for AP and AC inhibition of midazolam were 58.46  $\mu$ M and 8.20  $\mu$ M, respectively.

### Effect of AC on the Metabolism of Midazolam and Hydroxy-Midazolam in vivo

The pharmacokinetic parameters results revealed a significant difference between Group A and Group B ( $P < 0.05$ ) regarding the data of  $AUC_{(0-t)}$ ,  $AUC_{(0-\infty)}$ ,  $T_{max}$ ,  $V_z/F$ , and  $CL_z/F$  (Tables 4 and 5). Compared with Group A, Group B showed an increased  $T_{max}$  for midazolam (130%) and decreased  $V_z/F$  (43%),  $AUC$  (34%),  $CL_z/F$  (62%), and  $C_{max}$  (20%) (Tables 4 and 5 and Figure 4).

### Effect of AP on the Metabolism of Midazolam and Hydroxy-Midazolam in vivo

Similar Group B, Group C exhibited a large difference from Group A in  $AUC_{(0-t)}$ ,  $AUC_{(0-\infty)}$ ,  $T_{max}$ ,  $V_z/F$ , and  $CL_z/F$ . In detail, when AP was combined with midazolam, the  $AUC$  of midazolam increased by 55%,  $T_{max}$  increased by 217%,  $V_z/F$  decreased by 42%,  $CL_z/F$  decreased by 39%,  $C_{max}$  increased by 153%, and for hydroxy-midazolam, the  $AUC$  decreased by 41%,  $T_{max}$  increased

**Table 3** Accuracy, Precision and Extraction Recovery of Hydroxy-Midazolam and Midazolam in Rat Plasma (n=6)

Drug	Concentration (ng/mL)	RSD (%)		Accuracy (%)		Recovery (%)	Matrix Effect (%)
		Intra-Day	Inter-Day	Intra-Day	Inter-Day		
Hydroxy-midazolam	0.5	4.5	4.0	103.3	98.3	82.7	100.5
	8	4.6	1.9	98.7	99.4	83.9	96.8
	80	6.3	6.8	99.3	98.4	84.1	98.3
Midazolam	4	5.8	5.1	101.7	107	74.0	100.3
	45	1.2	3.5	101.6	100.8	76.7	97.7
	400	5.6	5.3	96.9	92.3	75.4	98.1

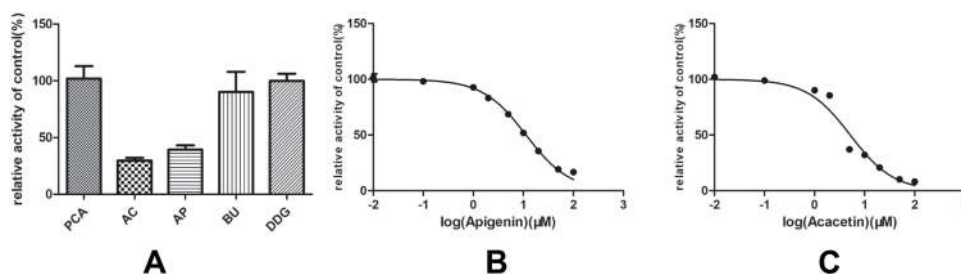


**Figure 3** (A) The inhibition ratios of five main components of *Lygodium* root on the metabolic activity of midazolam. (B) Inhibitory potential of AP on midazolam metabolism in RLMs. Results were presented at mean  $\pm$  SD (n = 3). (C) Inhibitory potential of AC on midazolam metabolism in RLMs. Results were presented at mean  $\pm$  SD (n = 3).

by 116%,  $V_{z/F}$  decreased by 43%,  $CL_{z/F}$  increased by 76%, and  $C_{max}$  decreased by 40%. The specific data were shown in Tables 4 and 5 and Figure 4.

## Discussion

In this study, a rapid, accurate and highly sensitive UPLC-MS/MS method was developed to detect PCA, AC, AP, BU and DDG in *Lygodium* root simultaneously. The established quantitative method is simple, time-saving, accurate and easy to handle and, thus, can be used for quality assessment and safety and toxicity evaluation of *Lygodium* root. In addition, a UPLC-MS/MS method for the detection of the CYP3A1 probe drug, midazolam, was also constructed and evaluated. Then, we established an in vitro analysis system by incubating rat microsomes with midazolam and a *Lygodium* root extract solution to evaluate whether PCA, AC, AP, BU and DDG could inhibit midazolam metabolism in vitro. As a result, we found that only AC and AP exhibited inhibitory effects on the

metabolism of midazolam. In addition, we also evaluated these inhibitory effects in rats by orally administering midazolam with AC or AP. As expected, the in vivo experiment corresponded well with previously observed in vitro data.

Cytochrome P450 (CYP) 3A subfamily plays a very important role in the metabolism of xenobiotics, with a very broad substrate specificity. In humans, CYP3A is divided into four subtypes: CYP3A4, CYP3A5, CYP3A7 and CYP3A43. These enzymes are mainly distributed throughout the liver and intestine.<sup>34</sup> In rats, six subtypes have been reported to date, which include CYP3A1, CYP3A2, CYP3A9, CYP3A18, CYP3A23 and CYP3A62.<sup>34–39</sup> Although the rat is not a good model for humans to study CYP3A4 induction, it is still reasonable to perform experiments using mice or male rats for CYP3A activity for comparison with humans, as the anti-rat CYP3A2 inhibition profile obtained in mice and male rats is most similar to the inhibition profile of human liver microsomes.<sup>40,41</sup>

**Table 4** Primary Pharmacokinetic Parameters of Midazolam After Oral Administration of Midazolam (10 mg/kg), AC and AP (5 mg/kg) in Rats (n = 6, Mean $\pm$ SD)

Parameters	Group A	Group B	Group C
AUC <sub>(0-t)</sub> ( $\mu\text{g h L}^{-1}$ )	240.39 $\pm 79.61$	328.63 $\pm 107.36$	372.69 $\pm 60.72^*$
AUC <sub>(0-\infty)</sub> ( $\mu\text{g h L}^{-1}$ )	248.68 $\pm 85.90$	330.88 $\pm 106.96$	378.15 $\pm 59.44^*$
$t_{1/2z}$ (h)	1.07 $\pm$ 0.34	0.80 $\pm$ 0.35	0.97 $\pm$ 0.17
$T_{max}$ (h)	0.29 $\pm$ 0.10	0.67 $\pm$ 0.26*	0.92 $\pm$ 0.20*
$V_z/F$ (L $\text{kg}^{-1}$ )	66.83 $\pm$ 24.73	38.33 $\pm$ 18.84*	38.50 $\pm$ 12.82*
$CL_z/F$ (L $\text{h}^{-1}$ $\text{kg}^{-1}$ )	44.59 $\pm$ 15.35	33.07 $\pm$ 10.71	27.05 $\pm$ 4.64*
$C_{max}$ ( $\mu\text{g L}^{-1}$ )	144.98 $\pm 39.00$	199.94 $\pm$ 62.51	222.30 $\pm 60.33^*$

**Note:** \* $P < 0.05$  indicates statistical difference between Group A, Group B and Group C.

**Abbreviations:** AC, acacetin; AP, apigenin; AUC, area under the plasma concentration-time curve;  $t_{1/2}$ , half-life;  $T_{max}$ , maximum plasma time; CL, plasma clearance;  $C_{max}$ , maximum plasma concentration.

**Table 5** Primary Pharmacokinetic Parameters of Hydroxy-Midazolam After Oral Administration of Midazolam (10 mg/kg), AC and AP (5 mg/kg) in Rats (n = 6, Mean $\pm$ SD)

Parameters	Group A	Group B	Group C
AUC <sub>(0-t)</sub> ( $\mu\text{g h L}^{-1}$ )	150.00 $\pm 32.47$	99.65 $\pm$ 28.00*	89.23 $\pm$ 27.41*
AUC <sub>(0-\infty)</sub> ( $\mu\text{g h L}^{-1}$ )	159.60 $\pm 35.74$	99.92 $\pm$ 27.99*	91.40 $\pm$ 27.55*
$t_{1/2z}$ (h)	1.35 $\pm$ 0.73	0.66 $\pm$ 0.10	1.07 $\pm$ 0.45
$T_{max}$ (h)	0.50 $\pm$ 0.00	0.58 $\pm$ 0.20*	1.08 $\pm$ 0.49*
$V_z/F$ (L $\text{kg}^{-1}$ )	120.68 $\pm 53.45$	104.78 $\pm$ 43.96	179.35 $\pm$ 84.40
$CL_z/F$ (L $\text{h}^{-1}$ $\text{kg}^{-1}$ )	66.14 $\pm$ 18.96	107.21 $\pm 31.33^*$	116.69 $\pm 29.64^*$
$C_{max}$ ( $\mu\text{g L}^{-1}$ )	79.09 $\pm$ 8.19	62.90 $\pm$ 18.65*	48.00 $\pm$ 14.75*

**Note:** \* $P < 0.05$  indicates statistical difference between Group A, Group B and Group C.

**Abbreviations:** AC, acacetin; AP, apigenin; AUC, area under the plasma concentration-time curve;  $t_{1/2}$ , half-life;  $T_{max}$ , maximum plasma time; CL, plasma clearance;  $C_{max}$ , maximum plasma concentration.



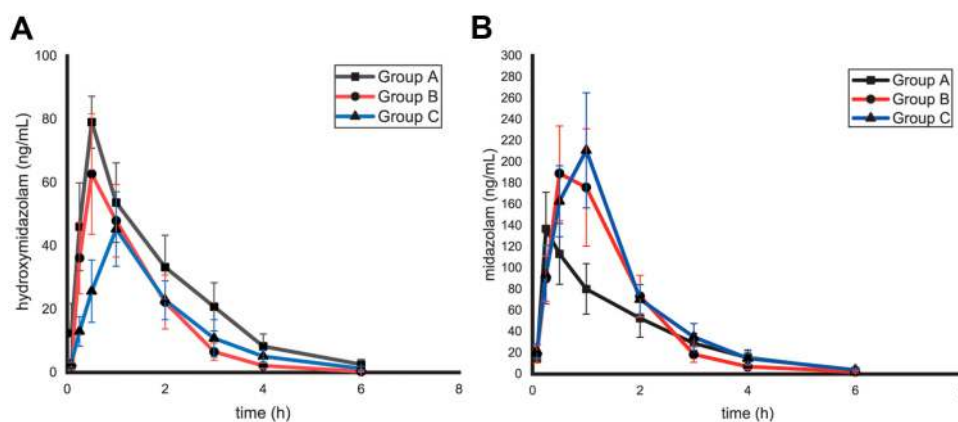


**Figure 4** (A) Mean plasma concentration-time profile of midazolam after oral administration of midazolam (10 mg/kg) in rats. Group A, Group B and Group C (n = 6, mean  $\pm$  SD). (B) Mean plasma concentration-time profile of hydroxy-midazolam after oral administration of midazolam (10 mg/kg) in rats. Group A, Group B and Group C (n = 6, mean  $\pm$  SD).

Midazolam is a well-known drug that is used to treat acute seizures and status epilepticus, including neurologically induced seizures and is mainly metabolized by the CYP3A/5 subtype (human) or CYP3A1/2 subtype (rat) in the liver.<sup>42</sup> In this study, we used midazolam as the probe drug for the inhibitory effect assessment *in vitro* and *in vivo*. As reported, the *in vitro* incubation method with RLMs is a reasonable biochemical reaction method for simulating the physiological environment.<sup>43–45</sup> Compared with other methods, for example, cell culture, this method exhibits many advantages, such as easy operation, less interfering factors, better reproducibility, intuitiveness and easy handling of multiple samples. In the pre-screening experiment of *Lygodium* root extraction, including 50  $\mu$ M midazolam, we found that only AC and AP had a strong influence on midazolam metabolism, especially AC. This result corresponded well with previously published reports that AP has an inhibitory effect on imatinib metabolized by CYP3A.<sup>46</sup> Additionally, *in vivo* data showed that the inhibitory effect of AC was stronger than that of AP.

Although RLMs incubation can reflect metabolism to a certain extent, it is still difficult to illustrate real metabolism in the human or animal body. In this study, we developed a UPLC-MS/MS method for the determination of the main components of *Lygodium* root in rat plasma and successfully applied it for the pharmacokinetic study of midazolam after oral administration. Compared with HPLC and UPLC,<sup>47,48</sup> the UPLC-MS/MS system showed several unique advantages: simple sample processing, high sensitivity, time-saving and so on. As shown in Tables 4 and 5, AP and AC significantly increased the AUC and reduced the CL of administered midazolam, which suggests that the metabolism of midazolam was

inhibited *in vivo* when combined with AP or AC. These results corresponded well with the incubation results *in vitro*. Specifically, *in vivo* data revealed that  $T_{max}$ ,  $C_{max}$  and  $MRT_{0-t}$  were significantly increased compared with the control group after combined medication. These data indicate that during long-term administration, it is necessary to appropriately adjust the dosage and frequency of administration of CYP3A4 drugs to prevent possible adverse reactions caused by inhibition of *Lygodium* root.

## Conclusion

In this study, a sensitive, time-saving UPLC-MS/MS method was developed for the simultaneous detection of midazolam and the main components of *Lygodium* root. Using this method, we found that AP and AC could inhibit the catalytic activities of midazolam *in vitro* and *in vivo*, indicating that much more attention should be paid when taking *Lygodium* root and midazolam synchronously in clinic.

## Data Sharing Statement

Raw data and figures of the current study are available as a dataset via Mendeley: <https://data.mendeley.com/datasets/52gxvdyym2/1>.

## Acknowledgments

The authors gratefully thank Prof. Dapeng Dai for his helpful writing-review and editing of the manuscript. This work was supported by grants funded by the Natural Science Foundation of Zhejiang and Zhejiang Pharmaceutical Association Joint Foundation (LYY18H280003), the High-Level Talent Training Project of Lishui (2015RC03 and 2018RC18), City-level public welfare technology application research project of

Lishui (No. 2016GYX42 and 2017GYX15) and CAMS Innovation Fund for Medical Sciences (2018-I2M-1-002).

## Disclosure

The authors report no conflicts of interest in this work.

## References

- Chen L, Zhang G, He J, et al. New naphthoquinone from the root of *Lygodium japonicum* (Thunb.) Sw. *J Nat Med*. 2010;64(1):114–116. doi:10.1007/s11418-009-0376-y
- Lee JA, Ha SK, Kim YC, Choi I. Effects of friedelin on the intestinal permeability and bioavailability of apigenin. *Pharmacol Rep*. 2017;69(5):1044–1048. doi:10.1016/j.pharep.2017.04.012
- Yang YC, Wei MC. Development and characterization of a green procedure for apigenin extraction from *Scutellaria barbata* D. Don. *Food Chem*. 2018;252:381–389. doi:10.1016/j.foodchem.2017.12.086
- Chen WP, Yang ZG, Hu PF, Bao JP, Wu LD. Acacetin inhibits expression of matrix metalloproteinases via a MAPK-dependent mechanism in fibroblast-like synoviocytes. *J Cell Mol Med*. 2015;19(8):1910–1915. doi:10.1111/jcmm.12564
- Jiang H, Yu J, Zheng H, et al. Breast cancer resistance protein and multi-drug resistance protein 2 regulate the disposition of acacetin glucuronides. *Pharm Res*. 2017;34(7):1402–1415. doi:10.1007/s11095-017-2157-8
- Zhao N, Dong Q, Fu XX, et al. Acacetin blocks kv1.3 channels and inhibits human T cell activation. *Cell Physiol Biochem*. 2014;34(4):1359–1372. doi:10.1159/000366343
- Abdel-Wahab MH, El-Mahdy MA, Abd-Ellah MF, Helal GK, Khalifa F, Hamada FM. Influence of p-coumaric acid on doxorubicin-induced oxidative stress in rat's heart. *Pharmacol Res*. 2003;48(5):461–465. doi:10.1016/S1043-6618(03)00214-7
- Yoon JH, Youn K, Ho CT, Karwe MV, Jeong WS, Jun M. p-coumaric acid and ursolic acid from corni fructus attenuated  $\beta$ -amyloid 25–35 induced toxicity through regulation of the NF- $\kappa$ B signaling pathway in PC12 cells. *J Agric Food Chem*. 2014;62(21):4911–4916. doi:10.1021/jf501314g
- Pragasam SJ, Venkatesan V, Rasool M. Immunomodulatory and anti-inflammatory effect of p-coumaric acid, a common dietary polyphenol on experimental inflammation in rats. *Inflammation*. 2013;36(1):169–176. doi:10.1007/s10753-012-9532-8
- Nasr Bouzaiane N, Kilani Jaziri S, Kovacic H, Chekir-Ghedira L, Ghedira K, Luis J. The effects of caffeic, coumaric and ferulic acids on proliferation, superoxide production, adhesion and migration of human tumor cells in vitro. *Eur J Pharmacol*. 2015;766:99–105. doi:10.1016/j.ejphar.2015.09.044
- Kot B, Wicha J, Piechota M, Wolska K, Gruzewska A. Antibiofilm activity of trans-cinnamaldehyde, p-coumaric, and ferulic acids on uropathogenic *Escherichia coli*. *Turk J Med Sci*. 2015;45(4):919–924. doi:10.3906/sag-1406-112
- Vauzour D, Corona G, Spencer JP. Caffeic acid, tyrosol and p-coumaric acid are potent inhibitors of 5-S-cysteinyldopamine induced neurotoxicity. *Arch Biochem Biophys*. 2010;501(1):106–111. doi:10.1016/j.abb.2010.03.016
- Lamba JK, Lin YS, Schuetz EG, Thummel KE. Genetic contribution to variable human CYP3A-mediated metabolism. *Adv Drug Deliv Rev*. 2002;54(10):1271–1294. doi:10.1016/S0169-409X(02)00066-2
- Robertson SM, Luo X, Dubey N, et al. Clinical drug-drug interaction assessment of ivacaftor as a potential inhibitor of cytochrome P450 and P-glycoprotein. *J Clin Pharmacol*. 2015;55(1):56–62. doi:10.1002/jcph.377
- van Dyk M, Marshall JC, Sorich MJ, Wood LS, Rowland A. Assessment of inter-racial variability in CYP3A4 activity and inducibility among healthy adult males of Caucasian and South Asian ancestries. *Eur J Clin Pharmacol*. 2018;74(7):913–920. doi:10.1007/s00228-018-2450-4
- Yang J, Patel M, Nikanjam M, et al. Midazolam single time point concentrations to estimate exposure and cytochrome P450 (CYP) 3A constitutive activity utilizing limited sampling strategy with a population pharmacokinetic approach. *J Clin Pharmacol*. 2018;58(9):1205–1213. doi:10.1002/jcph.1125
- Nicolas JM, Espie P, Molimard M. Gender and interindividual variability in pharmacokinetics. *Drug Metab Rev*. 2009;41(3):408–421. doi:10.1080/10837450902891485
- Wilkinson GR. Genetic variability in cytochrome P450 3A5 and in vivo cytochrome P450 3A activity: some answers but still questions. *Clin Pharmacol Ther*. 2004;76(2):99–103. doi:10.1016/j.clpt.2004.04.005
- Obreli Neto PR, Nobili A, de Lyra DP, et al. Incidence and predictors of adverse drug reactions caused by drug-drug interactions in elderly outpatients: a prospective cohort study. *J Pharm Pharm Sci*. 2012;15(2):332–343. doi:10.18433/J3CC86
- Fasinu PS, Bouic PJ, Rosenkranz B. An overview of the evidence and mechanisms of herb-drug interactions. *Front Pharmacol*. 2012;3:69. doi:10.3389/fphar.2012.00069
- Izzo AA, Ernst E. Interactions between herbal medicines and prescribed drugs: an updated systematic review. *Drugs*. 2009;69(13):1777–1798. doi:10.2165/11317010-000000000-00000
- Choi YH, Chin YW, Kim YG. Herb-drug interactions: focus on metabolic enzymes and transporters. *Arch Pharm Res*. 2011;34(11):1843–1863. doi:10.1007/s12272-011-1106-z
- Riss J, Cloyd J, Gates J, Collins S. Benzodiazepines in epilepsy: pharmacology and pharmacokinetics. *Acta Neurol Scand*. 2008;118(2):69–86. doi:10.1111/j.1600-0404.2008.01004.x
- Murthy JM. Refractory status epilepticus. *Neurol India*. 2006;54(4):354–358. doi:10.4103/0028-3886.28104
- Huf G, Alexander J, Gandhi P, Allen MH. Haloperidol plus promethazine for psychosis-induced aggression. *Cochrane Database Syst Rev*. 2016;11:CD005146. doi:10.1002/14651858.CD011360.pub2
- Brigo F, Nardone R, Tezzon F, Trinka E. Nonintravenous midazolam versus intravenous or rectal diazepam for the treatment of early status epilepticus: a systematic review with meta-analysis. *Epilepsy Behav*. 2015;49:325–336. doi:10.1016/j.yebeh.2015.02.030
- Hu LM, Lin GT, Zhang MM, Wang JF, Wang SH, Wang B. Pharmacokinetic study of syringin in rat by ultra-performance liquid-chromatography tandem mass spectrometry. *Lat Am J Pharm*. 2017;36(6):1231–1235.
- Huang P, Hua AL, Wang SZ, et al. Development of an UPLC-MS/MS validated method for determination and pharmacokinetic study of neratinib in rat plasma. *Lat Am J Pharm*. 2018;37(7):1392–1398.
- Liu J, Jin WQ, Lu XJ, Ye LX, Zhou YF, Ruan LN. Determination of triptophenolide in rat plasma by UPLC-MS/MS and its pharmacokinetics. *Lat Am J Pharm*. 2018;37(5):893–897.
- Ma JS, Wang SH, Huang XL, et al. Validated UPLC-MS/MS method for determination of hordenine in rat plasma and its application to pharmacokinetic study. *J Pharm Biomed Anal*. 2015;111:131–137. doi:10.1016/j.jpba.2015.03.032
- Ma JS, Wang SH, Zhang ML, et al. Simultaneous determination of bupropion, metoprolol, midazolam, phenacetin, omeprazole and tolbutamide in rat plasma by UPLC-MS/MS and its application to cytochrome P450 activity study in rats. *Biomed Chromatogr*. 2015;29(8):1203–1212. doi:10.1002/bmc.3409
- Wang XQ, Wang SH, Ma JS, et al. Pharmacokinetics in rats and tissue distribution in mouse of berberrubine by UPLC-MS/MS. *J Pharm Biomed Anal*. 2015;115:368–374. doi:10.1016/j.jpba.2015.07.031
- Wang SH, Wu HY, Geng PW, et al. Pharmacokinetic study of denobine in rat plasma by ultra-performance liquid chromatography tandem mass spectrometry. *Biomed Chromatogr*. 2016;30(7):1145–1149. doi:10.1002/bmc.3641

34. Martignoni M, Groothuis GM, de Kanter R. Species differences between mouse, rat, dog, monkey and human CYP-mediated drug metabolism, inhibition and induction. *Expert Opin Drug Metab Toxicol.* 2006;2(6):875–894. doi:10.1517/17425255.2.6.875
35. Wang H, Kawashima H, Strobel HW. cDNA cloning of a novel CYP3A from rat brain. *Biochem Biophys Res Commun.* 1996;221(1):157–162. doi:10.1006/bbrc.1996.0562
36. Gonzalez FJ, Nebert DW, Hardwick JP, Kasper CB. Complete cDNA and protein sequence of a pregnenolone 16 alpha-carbonitrile-induced cytochrome P-450. A representative of a new gene family. *J Biol Chem.* 1985;260(12):7435–7441.
37. Gonzalez FJ, Song BJ, Hardwick JP. Pregnenolone 16 alpha-carbonitrile-inducible P-450 gene family: gene conversion and differential regulation. *Mol Cell Biol.* 1986;6(8):2969–2976. doi:10.1128/MCB.6.8.2969
38. Strotkamp D, Roos PH, Hanstein WG. A novel CYP3 gene from female rats. *Biochim Biophys Acta.* 1995;1260(3):341–344. doi:10.1016/0167-4781(94)00244-W
39. Kirita S, Matsubara T. cDNA cloning and characterization of a novel member of steroid-induced cytochrome P450 3A in rats. *Arch Biochem Biophys.* 1993;307(2):253–258. doi:10.1006/abbi.1993.1587
40. Bogaards JJ, Bertrand M, Jackson P, et al. Determining the best animal model for human cytochrome P450 activities: a comparison of mouse, rat, rabbit, dog, micropig, monkey and man. *Xenobiotica.* 2000;30(12):1131–1152. doi:10.1080/00498250010021684
41. Zuber R, Anzenbacherova E, Anzenbacher P. Cytochromes P450 and experimental models of drug metabolism. *J Cell Mol Med.* 2002;6(2):189–198. doi:10.1111/j.1582-4934.2002.tb00186.x
42. Olsen LR, Gabel-Jensen C, Wubshet SG, et al. Characterization of midazolam metabolism in locusts: the role of a CYP3A4-like enzyme in the formation of 1'-OH and 4-OH midazolam. *Xenobiotica.* 2016;46(2):99–107. doi:10.3109/00498254.2015.1051604
43. Wang Q, Dai Z, Wen B, Ma S, Zhang Y. Estimating the differences of UGT1A1 activity in recombinant UGT1A1 enzyme, human liver microsomes and rat liver microsome incubation systems in vitro. *Biol Pharm Bull.* 2015;38(12):1910–1917. doi:10.1248/bpb.b15-00513
44. Palacharla RC, Uthukam V, Manoharan A, et al. Inhibition of cytochrome P450 enzymes by saturated and unsaturated fatty acids in human liver microsomes, characterization of enzyme kinetics in the presence of bovine serum albumin (0.1 and 1.0% w/v) and in vitro - in vivo extrapolation of hepatic clearance. *Eur J Pharm Sci.* 2017;101:80–89. doi:10.1016/j.ejps.2017.01.027
45. Kim JH, Kim HS, Kong TY, et al. In vitro metabolism of a novel synthetic cannabinoid, EAM-2201, in human liver microsomes and human recombinant cytochrome P450s. *J Pharm Biomed Anal.* 2016;119:50–58. doi:10.1016/j.jpba.2015.11.023
46. Liu XY, Xu T, Li WS, et al. The effect of apigenin on pharmacokinetics of imatinib and its metabolite N-desmethyl imatinib in rats. *Biomed Res Int.* 2013;2013:789184. doi:10.1155/2013/789184
47. Jurica J, Dostalek M, Konecny J, Glatz Z, Hadasova E, Tomandl J. HPLC determination of midazolam and its three hydroxy metabolites in perfusion medium and plasma from rats. *J Chromatogr B Analyt Technol Biomed Life Sci.* 2007;852(1–2):571–577. doi:10.1016/j.jchromb.2007.02.034
48. Elbarbry F, Attia A, Shoker A. Validation of a new HPLC method for determination of midazolam and its metabolites: application to determine its pharmacokinetics in human and measure hepatic CYP3A activity in rabbits. *J Pharm Biomed Anal.* 2009;50(5):987–993. doi:10.1016/j.jpba.2009.07.004

## Drug Design, Development and Therapy

Dovepress

### Publish your work in this journal

Drug Design, Development and Therapy is an international, peer-reviewed open-access journal that spans the spectrum of drug design and development through to clinical applications. Clinical outcomes, patient safety, and programs for the development and effective, safe, and sustained use of medicines are a feature of the journal, which has also

been accepted for indexing on PubMed Central. The manuscript management system is completely online and includes a very quick and fair peer-review system, which is all easy to use. Visit <http://www.dovepress.com/testimonials.php> to read real quotes from published authors.

Submit your manuscript here: <https://www.dovepress.com/drug-design-development-and-therapy-journal>